Study of Intermittent Bifurcations and Chaos in Buck-Boost Converters with Input regulators

C.D. Xu[1], K.W.E. Cheng[1*], H. Zhang[2], X. K. Ma[2], K. Ding[1]
[1]Department of Electrical Engineering, The Hong Kong Polytechnic University, Hong Kong, China
[2]School of Electrical Engineering, Xi'an Jiaotong University, Shaanxi, China
E-mail: eeecheng@polyu.edu.hk

Abstract - This paper presents two series of models in the buck-boost converters with input regulators under peak current mode control. Stroboscopic maps are derived to describe the dynamical behaviors of buck-boost converters with input filter capacitor. In terms of the developed discrete maps, fast scale instabilities in buck-boost converters are studied. Numerical results reveal the circuit system exhibits distinguishing nonlinear phenomena, i.e., intermittent bifurcations and chaos. In addition, the periodicity of the intermittent behaviors is also analyzed in detail.

INTRODUCTION

Input capacitor is one of the most widely used regulators to rectify the input voltage in many kinds of converters and has a large application literature. This motivates the requirement for a deeper understanding of their dynamical behavior and further explorations of some operation modes. Our major motivation of our work is not only to improve their performances such as stability region, efficiency, EMC, etc., but also to find the new fields of application[1-3]. Thus, the investigation of the dynamics of buck-boost converters with input regulators, especially seek possible applications that are of direct relevance of industrial power electronics has become one of the most interesting subjects of much on-going research in this field. In recent years, there has been much effort in dynamical behavior analysis of the DC/DC converters[4-9]. The elaborate analysis and results based on the buck converter, the boost converter, and the buck-boost converter has been presented in both experimental and theoretical simulation, which led to a better understanding of the dynamics in the converters. However, most of the results are based of the ideal dc input voltage. In contrast, the dc voltage is transformed by the ac voltage with a regulator in the practical engineering application, which produces an interaction on the converter. Some researchers [3, 10-12] have carried on the interaction problem between input regulator and the power system, most of results and studies are also on the assumption that the input is ideal dc power supply. Whereas they still give us some clues to improve our method of researching in this field, which show that the small-signal averaged model widely used in the design of DC/DC regulators does not provide a complete understanding of the stability of the filter-regulator system. The large-signal time domain nonlinear averaged model is used to furthering understand the interaction on the slow scale using nonlinear analysis techniques. No fast scale interactions, however, can be predicted using this model. Since the nonlinear dynamics depend not only on the switching frequency variation, but also on the periodicity of the input voltage, it is evident that precisely discrete maps modeling is thus needed to investigate the dynamical behavior of the converter with input rectifier on fast scale.

In this paper, we consider stroboscopic maps to model buck-boost converters with input regulator under peak-current mode control. In view of the complexity of the circuit systems, two series of nonlinear discrete maps are derived to describe exactly the nonlinear dynamics of the systems. Based on the developed models, we can present some numerical simulation results to investigate the evolution process of intermittent behavior and the periodicity of intermittency in the circuit systems, the occurrence of intermittent bifurcations and chaos with half one line period, the effect of the variation of the input capacitance. The study provides clear direction to identify the fast scale instability and the effect of the input capacitor on the buck-boost converter.

SYSTEM DESCRIPTION AND NONLINEAR DISCRETE MAPS

A typical buck-boost converter with input regulator is shown in Figure 1. We assume throughout that the components in the circuit are ideal and no parasitic effects are considered.

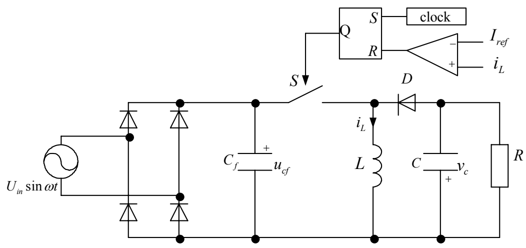

Fig.1. Schematics of buck-boost converter with input regulators

The circuit is governed by two fundamental parts, the regulator transforms ac to dc, the others transforms dc to dc. Since the rectifier bridge exists, the current can not reverse to flow into the power system, at the same time there are two kinds of conditions, $|U_{in}\sin\omega nT_s| > u_{cf}(nT_s)$ or $|U_{in}\sin\omega nT_s| < u_{cf}(nT_s)$, and then the circuit can be divided into two sets of models, one is state 1 and state 2, while $|U_{in}\sin\omega nT_s| > u_{cf}(nT_s)$, the other is state 3 and state 4, while $|U_{in}\sin\omega nT_s| < u_{cf}(nT_s)$. In this study, stroboscopic mapping is used to model the power converter systems and obtains the state variables. i.e., the inductor current i, the input capacitor voltage u_{cf}, the output voltage v_c, which are periodically sampled at a fixed time interval T_s. The state variables i_{n+1}, v_{n+1}, u_{n+1} are the beginning states at the (n+1) switching period, which can be calculated by the previous sampling instant value i_n, v_n, u_n.

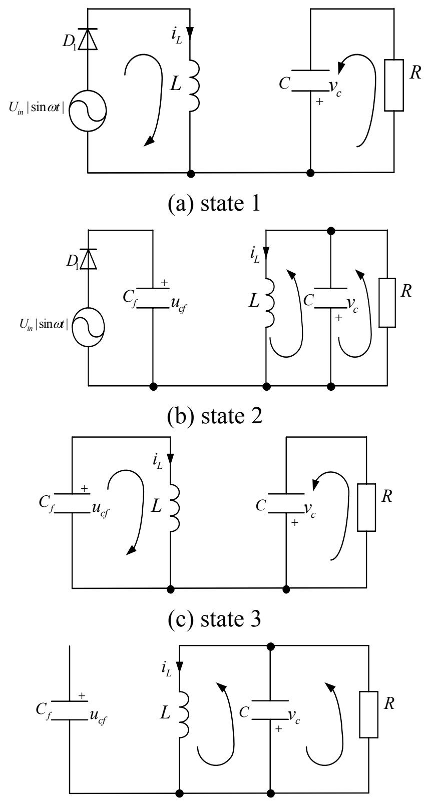

(a) state 1

(b) state 2

(c) state 3

(d) state 4

Fig. 2. The operation of the circuit.

On the assumption that the initial state $|U_{in}\sin\omega nT_s| > u_{cf}(nT_s)$ at the nth switching cycle under peak current mode control, the transistor is turned on, the circuit operates in the state 1 as shown in Fig.2(a), it is turned off while the inductor current reaches the reference current, and the circuits operate in state 2 as shown in Fig. 2(b); if $|U_{in}\sin\omega nT_s| < u_{cf}(nT_s)$ at the nth switching cycle, the transistor is turned on, the circuit operates in state 3 as shown in Fig. 2(c), the switch is turned off while the inductor current reaches reference current, the circuit operates in state 4 as shown in Fig. 2(d). Then the equations can be obtained as follows.

State 1: S is on, D is off, $|U_{in}\sin\omega t| > u_{cf}(t)$.

$$\begin{cases} \dfrac{di_L}{dt} = \dfrac{U_{in}|\sin\omega t|}{L} \\ u_{cf} = U_{in}|\sin\omega t| \quad (\omega = 2\pi f_l) \\ \dfrac{dv_C}{dt} = -\dfrac{v_C}{RC} \end{cases} \tag{1}$$

State 2: S is off, D is on, $U_{in}|\sin\omega t| > u_{cf}(t)$

$$\begin{cases} \dfrac{di_L}{dt} = -\dfrac{v_C}{L} \\ u_{cf} = U_{in}|\sin\omega t| \quad (\omega = 2\pi f_l) \\ \dfrac{dv_C}{dt} = \dfrac{i_L}{C} - \dfrac{v_C}{RC} \end{cases} \tag{2}$$

State 3: S is on, D is off, $U_{in}|\sin\omega t| < u_{cf}(t)$

$$\begin{cases} \dfrac{di_L}{dt} = \dfrac{u_{cf}}{L} \\ \dfrac{du_{cf}}{dt} = -\dfrac{i_L}{C_f} \\ \dfrac{dv_C}{dt} = -\dfrac{v_C}{RC} \end{cases} \tag{3}$$

State 4: S is off, D is on, $U_{in}|\sin\omega t| < u_{cf}(t)$

$$\begin{cases} u_{cf} = u_{cf0} \\ \dfrac{di_L}{dt} = -\dfrac{v_C}{L} \\ \dfrac{dv_C}{dt} = \dfrac{i_L}{C} - \dfrac{v_C}{RC} \end{cases} \tag{4}$$

On the assumption that $S = \theta \bmod 2k\pi$, $k = 0,1,2,3...$, $\theta = \omega t, \theta \in [0, 2\pi]$,

then $S = \begin{cases} 1 & \theta \in [0, \pi) \\ -1 & \theta \in (\pi, 2\pi] \end{cases}$.

t_{n1}, t_{n2} are time intervals needed to reach the reference current corresponding to the state 1 and state 3 respectively, t_d is the time interval needed to reach the zero in state 2 and state 4. t_{n1}, t_{n2}, t_d are decided by the equation (5), (6), (7).

$$i_n + \frac{SU_m t_{n2}\sin\omega nT_s}{L} = I_{ref} \tag{5}$$

$$C_1\cos\beta(nT_s + t_{n1}) + C_2\sin\beta(nT_s + t_{n1}) = I_{ref} \tag{6}$$

$$e^{\alpha t_d}[C_1\cos\beta(nT_s + t_d) + C_2\sin\beta(nT_s + t_d)] = 0 \tag{7}$$

If at the beginning of nth switching cycle, $|U_{in}\sin\omega nT_s| > u_{cf}(nT_s)$ and $t_{n1} > T_s$, then at the time interval $[nT_s, (n+1)nT_s]$, the system operates in state 1, the state variables are calculated by the equation as follows

$$\begin{cases} i_{n+1} = i_n + \dfrac{SU_{in}\sin\omega nT_s}{L}T_s \\ u_{n+1} = SU_{in}\sin\omega(n+1)T_s \\ v_{n+1} = v_n e^{-T_s/RC} \end{cases} \tag{8}$$

If $t_{n1} < T_s$, at the time interval $[nT_s + t_{n1}, (n+1)nT_s]$, the system operates in state 2, the state variables can be calculated by the equation as follows

$$\begin{cases} i_{n+1} = e^{\alpha(T_s - t_n)}[C_1\cos\beta(n+1)T_s + C_2\sin\beta(n+1)T_s] \\ v_{n+1} = -Le^{\alpha(T_s - t_n)}[(C_1\alpha + C_2\beta)\cos\beta(n+1)T_s \\ \qquad + (C_2\alpha - C_1\beta)\sin\beta(n+1)T_s] \\ u_{n+1} = SU_{in}\sin\omega(n+1)T_s \end{cases} \tag{9}$$

where $C_1 = \cos\beta(nT_s + t_n) + \dfrac{\alpha}{\beta}\sin\beta(nT_s + t_n)i_{t_n} + \dfrac{\sin\beta(nT_s + t_n)}{L\beta}v_{t_n}$

$$C_2 = \sin\beta(nT_s + t_n) - \frac{\alpha}{\beta}\cos\beta(nT_s + t_n) i_{t_n} + \frac{\cos\beta(nT_s + t_n)}{L\beta} v_{t_n},$$

$\alpha = -1/2RC$, $\beta = \sqrt{\frac{4R^2C}{L} - 1/2RC}$.

If at the beginning of nth switching cycle $|U_{in}\sin\omega nT_s| < u_{cf}(nT_s)$, $t_{n2} > T_s$, at the time interval $[nT_s, (n+1)nT_s]$, the system operates in state 3, the state variables are calculated by the equation as follows:

$$\begin{cases} i_{n+1} = C_1\cos\beta(n+1)T_s + C_2\sin\beta(n+1)T_s \\ u_{n+1} = L\beta(C_2\cos\beta(n+1)T_s - C_1\sin\beta(n+1)T_s) \\ v_{n+1} = v_n e^{-T_s/RC} \end{cases} \quad (10)$$

where,

$C_1 = i_n\cos\beta nT_s - u_n\sin\beta nT_s / L\beta$,

$C_2 = i_n\sin\beta nT_s + u_n\cos\beta nT_s / L\beta$, $\beta = \sqrt{1/LC_f}$.

If $|U_m\sin\omega nT_s| < u_{cf}(nT_s)$, $t_{n2} < T_s$, at the time interval $[nT_s + t_{n2}, (n+1)nT_s]$, the system operates in state 4, the state variables can be calculated by the equation as follows:

$$\begin{cases} i_{n+1} = e^{\alpha(T_s - t_n)}[C_1\cos\beta(n+1)T_s + C_2\sin\beta(n+1)T_s] \\ v_{n+1} = -Le^{\alpha(T_s - t_n)}[(C_1\alpha + C_2\beta)\cos\beta(n+1)T_s \\ \qquad + (C_2\alpha - C_1\beta)\sin\beta(n+1)T_s] \\ u_{n+1} = u_{tn} \end{cases} \quad (11)$$

where, $C_1 = \cos\beta(nT_s + t_n) + \frac{\alpha}{\beta}\sin\beta(nT_s + t_n) i_{t_n} + \frac{\sin\beta(nT_s + t_n)}{L\beta} v_{t_n}$,

$$C_2 = \sin\beta(nT_s + t_n) - \frac{\alpha}{\beta}\cos\beta(nT_s + t_n) i_{t_n} + \frac{\cos\beta(nT_s + t_n)}{L\beta} v_{t_n},$$

$\alpha = -1/2RC$, $\beta = \sqrt{\frac{4R^2C}{L} - 1/2RC}$.

The equations (8), (9), (10), (11) describe precisely the operation of buck-boost converter with input regulator under the peak current mode control.

COMPUTER SIMULATION

Since input regulator is widely used to rectify input voltage, different input capacitor is given to research the dynamical behavior for buck-boost converter under peak current mode control with input regulator. We begin with a set of computer simulation to identify possible bifurcation phenomena. Numerical results are given based of the stroboscopic maps as follows. The parameters of the circuit is given as $T_s = 10\mu s$, $T = 20ms$, $L = 0.1mH$, $C = 100\mu F$, $R = 40\Omega$, $I_{ref} = 1.6A$, $U_{in} = 35V$.

For a certain set of parameters, fast scale instability may occur within half line cycle. Such instability may manifest itself as a rout to chaos at the switching frequency.

We give the simulation results of inductor current waveform for the different input capacitor as shown in Fig. 3(a-d), when the circuit operates stable. Fig. 3(a) shows the stable operation of period one in the whole half line cycle with $C_f = 220uF$. Fig. 3(b) shows bifurcation of period two in some intervals of half line cycle with $C_f = 150uF$. Fig. 3(c) shows bifurcation region in some time interval becomes larger with $C_f = 120uF$ than Fig. 3(b). Fig. 3(d) shows fast scale instability within half line cycle with $C_f = 90uF$. From above results we can obtain that the system operates periodically. In order to observe clearly the change in dynamical behavior, we sample the data in each switching cycle based on the stroboscopic maps derived above. Fig. 4(a-d) shows the corresponding calculated data in each switching cycle. It is obvious that it operates stable in period one shown in Fig. 4(a), and bifurcation of period two occurs at the beginning of each half line cycle shown in Fig. 4(b). Bifurcation of period two and period four occurs at the beginning of each half line cycle shown in Fig. 4(c). Specifically we can see the rout of period doubling to chaos from Fig. 4(d). The phase portrait is given as Fig. 5(a-d) respectively. It is clearly observed that the dynamical behavior in accordance with Fig. 3(a-d) respectively.

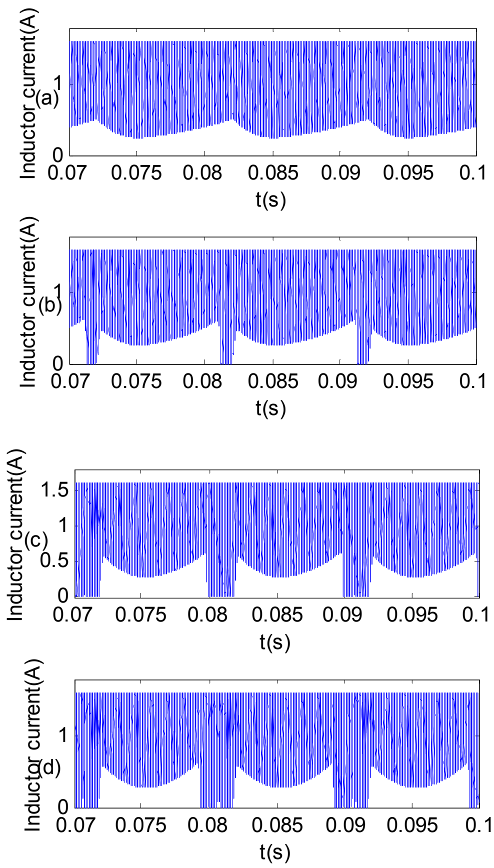

Fig. 3. (a)-(d) Time-domain wave-form of inductor current for $C_f = 220uF$, $C_f = 150uF$, $C_f = 120uF$ and $C_f = 90uF$.

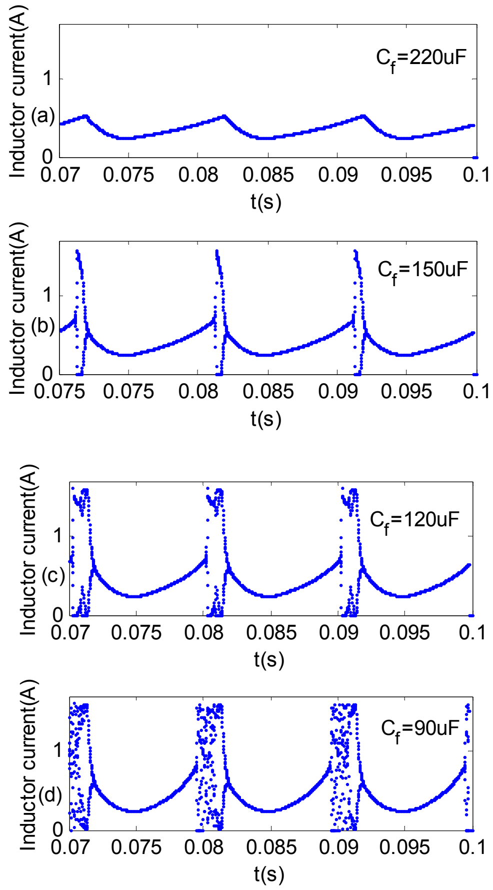

Fig. 4. (a)-(d) sampled data wave-form of inductor current for $C_f = 220uF$, $C_f = 150uF$, $C_f = 120uF$ $C_f = 90uF$.

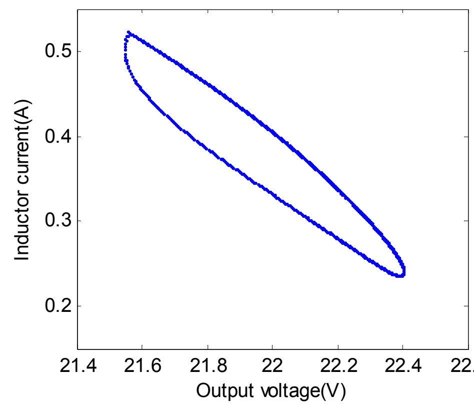

(a)

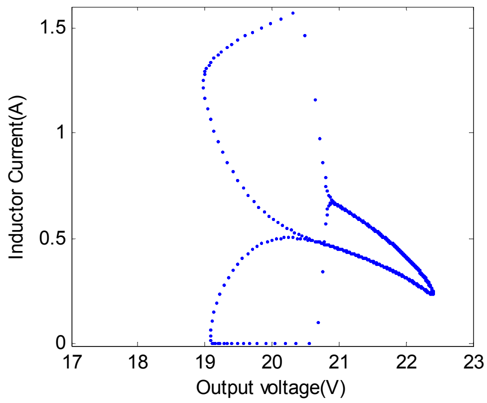

(b)

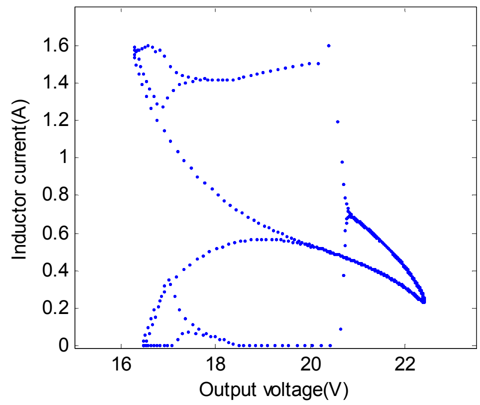

(c)

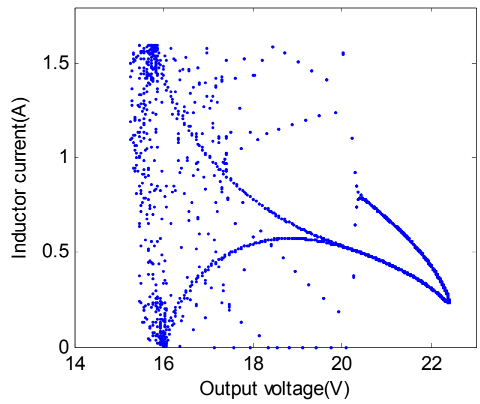

(d)

Fig. 5 (a)-(d) Phase portraits of sampled *i* versus v_c for $C_f = 220uF$, $C_f = 150uF$, $C_f = 120uF$, $C_f = 90uF$ respectively.

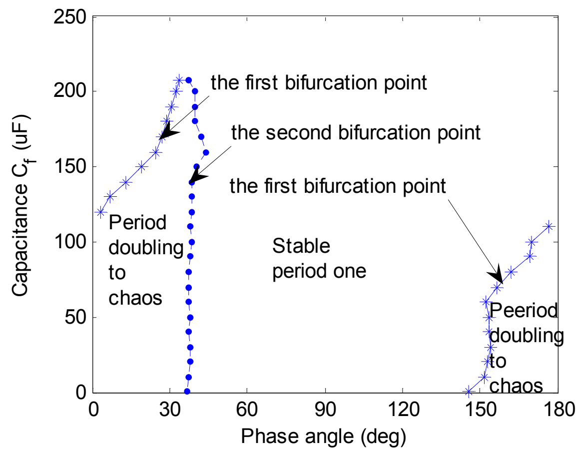

Fig. 6. Capacitance versus critical phase angles in half line cycle

It is noticed that complete asymmetry and periodic instability exist in a half line cycle, which we can easily obtain from Fig. 4. In order to figure out the nonlinear dynamics of the system, the investigation on the stable region is given as shown in Fig. 6. It is clear that the region of stable period one decreases when the capacitor decreases. Especially, when the capacitance is smaller than 120 uF , the unstable region is divided into two parts from one, that is, the first bifurcation point jumps over half line cycle and makes unstable region larger and we also can see that the second bifurcation point is nearly vertical, which can be observed in the Fig. 7. The inductor current and the rectifier voltage are given to investigate the detail of the dynamic characters as shown in Fig. 7 when $C_f = 120uF$ during a line period. We can easily observe the first bifurcation point and the second bifurcation point occurs in the part of section one when the system operates in the state 3 and 4 and the part of section two when the system operates in the state 1 and 2 respectively. As is known, when the system operates state 3 and 4, the rectifier voltage becomes smaller with the input capacitor decreasing, so that the first bifurcation point as shown in Fig. 7 moves left till jumping over the half line cycle and divides the unstable region into two parts and makes the unstable region larger in half line cycle as shown in Fig. 6. The second bifurcation point is nearly vertical as shown in Fig. 6. The reason is that the second bifurcation occurs in the period that the system operates state 1 and 2; when the rectifier voltage doesn't change with the input capacitor decreasing, so that the second bifurcation point nearly don't change, at that time the capacitance have no effect on the system as shown in Fig.6. We can easily understanding the fast scale instability of the system as shown in Fig.6 and Fig. 7.

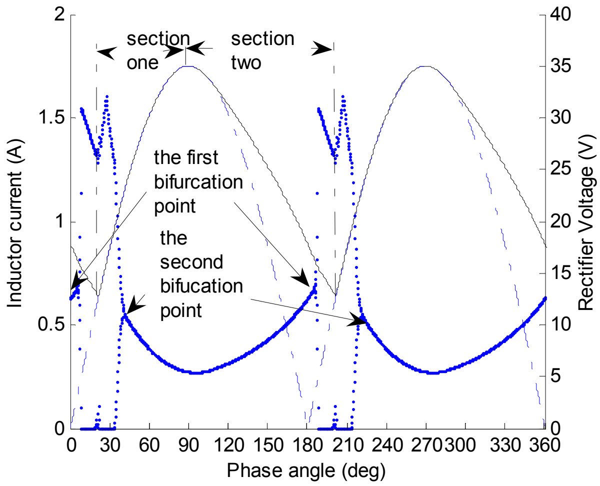

Fig. 7. The inductor current and the rectifier voltage when $C_f = 120uF$

CONCLUSION

In this paper, we have investigated the fast scale instability using precisely discrete maps for the buck-boost converter with input regulator, which lead a full understanding of the converter with rectifier and the interaction between the regulator and the system. Numerical simulations have been performed to study intermittent bifurcations and chaos in the circuit system, which show that fast scale instability results in intermittent bifurcations and chaos, the period of intermittency is equal to half of the one-line period and the input regulator can make the stable system into unstable even could damage the system, and also can make the stable arrange larger. Deep research will be developed on the border investigation on the input regulator and the bifurcation prediction, which help engineers to design the input regulator or input filter.

ACKNOWLEDGEMENTS

The authors would like to thank the colleagues giving helpful comments and suggestions.

REFERENCE

[1] Ma, X.K. and Zhang, H.: 'study of intermittent bifurcations and chaos in boost PFC converters by nonlinear discrete models', Chaos, solitons & fractals, 23, (2), 2005, pp. 431-444.

[2] Mazumder, S.K.; Nayfeh, A.H. and Borojevic, D.: 'Theoretical and experimental investigation of the fast and slow-scale instabilities of a DC-DC converter', IEEE Trans. Power Electron., 16, (2), 2001, pp. 201-216.

[3] Tse, C. K.: 'Complex Behavior of Power Electronics and Applications to Practical Design: An Overview', Special Report, 2004.

[4] Mazumder, S.K.; Nayfeh, A.H.; and Borojevic, D.: 'Stability analysis of parallel DC-DC converters using a nonlinear approach', IEEE, 2001, pp. 1284-1288.

[5] Cheng, K.W.E; Liu, M. and Wu, J.: 'Experimental study of bifurcation and chaos in the buck-boost converter', IEE Proc.-Electr. Power Appl., 150, (1), 2003, pp. 45-61.

[6] Tse, C.K. and Iu, H.H.C.: 'Bifurcation Behavior of Parallel-Connected Boost Converters', Int, J. Circ. Theor. Appli., 29, (3), 2001, pp. 281-298.

[7] Tan, F.D.; Ramshaw, R.S.: 'Instabilities of a boost converter system under large parameter variations', IEEE Trans. Power Electron., 4, (4), 1989, pp. 442-449.

[8] Cheng, K.W.E.; Liu, M. and Wu, J.: 'Chaos study and parameter-space analysis of the DC-DC buck-boost converter', IEE Proc.-Electr. Power Appl., 150, (2), 2003, pp. 126-138.

[9] Cheng, K.W.E and Liu, M.: 'Analysis and experimental verification of the linear correlation of the operation condition among the bifurcation points of the current-mode-controlled buck-boost converter', Int, J. Circ. Theor. Appli., 33, (1), 2005, pp. 99-108.

[10] Suntio, T. and Gadoura I.: 'Input filter interactions in peak-current-mode-controlled buck converter operating in CICM', IEEE Trans. On Indust. Electron., 49, (1), 2002, pp. 76-86.

[11] Dongsoo, K.; Choi, B.; Lee, D. and Sun, J.: 'Analysis of input filter interactions in switching power converters', Appl. Power Electron. Conferen. and Exposit.,Twentieth 2005. Ann. IEEE, 1, 2005, pp 191-198.

[12] Alfayyoumi, M.; Nayfeh, A.H. and Borojevic, D.: 'Input filter interactions in DC-DC switching regulators', Power Electron. Special. Conferen. PESC 99. 30th Ann. IEEE 1999. pp 926-932.